STUDIA UNIVERSITATIS BABEŞ-BOLYAI, CHEMIA, XLV, 2, TOM I, 2010

Dedicated to the memory of Prof. dr. Ioan Silaghi-Dumitrescu marking 60 years from his birth

GROWTH RATE OF HYDROXYAPATITE CRYSTALS OBTAINED BY PRECIPITATION

VALENTINA ROXANA DEJEU*, BARABÁS REKA, ANA-MARIA CORMOŞ, BOGYA ERZSÉBET SÁRA, PAUL-ŞERBAN AGACHI

ABSTRACT. Identification of a precipitation process consists in the formulation of a mathematical model which describes the real system characteristics. The model parameters have physical significance in terms like growth rate, nucleation rate or population density of particles. In the present work, the precipitation kinetics of hydroxyapatite (HAP) was studied at the laboratory scale using a 0.5 L batch reactor. The vessel was operated continuously at 25 ºC and 50 ºC at different feed concentrations. A methodology already known for other systems was applied to determine the kinetic parameters (growth rate) from the crystal size distribution (CSD) in the preparation of hydroxyapatite. Predicted particle size characteristics shown reasonable agreement with experimental data collected. The influence of feed concentration on particle size of hydroxyapatite was discussed too.

Keywords: *hydroxyapatite, growth rate, population balance, precipitation, particle formation, mathematical*

INTRODUCTION

The study of precipitation processes using chemical reaction engineering is based on a direct correlation between the processes kinetic (chemical reaction rates, nucleation and growth rates) and the final product quality (crystal shape and CSD). The way that this estimation is made is essential in the critical analysis of the accuracy and model validity. Several authors have presented methods for the simultaneous estimation of crystal growth and nucleation kinetics from batch crystallizations. In an early study, Bransom and Dunning (1949) derived a crystal population balance to analyse batch CSD for growth and nucleation kinetics. Misra and White (1971), Ness and White (1976) and McNeil et al. (1978) applied the population balance

* *Universitatea Babeş-Bolyai, Facultatea de Chimie şi Inginerie Chimică, Str. Kogălniceanu Nr. 1, RO-400084 Cluj-Napoca, Romania, vdejeu@chem.ubbcluj.ro*

to obtain both nucleation and crystal growth rates from the measurement of crystal size distributions during a batch experiment. In a refinement, Tavare and Garside (1986) applied the laplace transformation to the population balance. Qui and Rasmusson (1991) and Nvlt (1989), respectively, measured solution concentration during seeded batch cooling crystallizations and determined the crystal size distribution from which growth and nucleation rates were determined. Witkowski et al. (1990) used a non-linear parameter estimation technique to estimate nucleation and growth rates based on solution concentration and light obscuration measurements. Gutwald and Mersmann (1990) estimated growth and nucleation rates from constant supersaturation controlled batch crystallization. Qui and Rasmuson (1994) proposed a direct optimization method based on solution concentration and product CSD data from seeded batch experiments. Aoun etal. (1999) reviewed methods for determining precipitation kinetics and also presented a method for the simultaneous determination of growth and nucleation kinetics from batch experiments [1].

The precipitation of calcium phosphates has attracted the interest of many researches because of its importance in industrial water system scale formation (e.g. heat exchangers, cooling towers, boilers, etc.), in water treatment processes, in catalysis as supporting material, in agriculture as fertilizers, and basically in bio-mineralization processes [2, 3, 4]. Hydroxyapatite, thermodynamically the most stable calcium phosphate at pH > 5, is the main inorganic compound of hard tissues in vertebrates. Although the precipitation of HAP is of particular importance in the bio-mineralization processes, very little is known about the crystal growth mechanism [5].

In the present work, the precipitation kinetics and the influence of feed concentration on particle size of hydroxyapatite was studied at the laboratory scale. Kinetic parameters identification was realized using an optimization algorithm based on a least squares minimization.

Precipitation kinetics

For a global treatment of the growing phenomena is necessary to model the crystal size distribution using the population balance equation (PBE) [6, 7]. General form of PBE described by Randolph and Larson [8] is:

$$\frac{\partial n}{\partial t} + G\frac{\partial n}{\partial L} = B_{aggl} + B_{disr} - D_{aggl} - D_{disr} - \frac{nQ}{V} \tag{1}$$

where the birth terms for agglomeration and disruption are:

$$B_{aggl} + B_{disr} = \frac{L^2}{2}\int \frac{K_{aggl}\, n(L_u)n(L_v)dL_u}{L_v^2} + \int K_{disr} S(L_u, L_v)n(L_u)n(L_v)dL_u \tag{2}$$

and the death terms for agglomeration and disruption are:

$$D_{aggl} + D_{disr} = n(L)\int K_{aggl} n(L_u) dL_u + K_{disr} n(L) \tag{3}$$

The expression for the supersaturation was found to be:

$$S = \left(\frac{C_A^{\nu_A} C_B^{\nu_B}}{K_{sp}} \right)^{1/(\nu_A+\nu_B)} \tag{4}$$

Crystal growth rate data from industrial crystallizers are usually correlated empirically with environmental conditions, such as concentration and temperature using a power law model of the form:

$$G = k_g (\sigma + 1)^g \tag{5}$$

The power coefficient g in the growth equation does not depend on the form of the equation used and is normally a number between 1 and 2. The constants g and k_g are temperature-dependent and are usually fit to the Arrhenius equation to obtain a general expression for growth rate as a function of temperature. The Arrhenius equation can be written as:

$$k_g = A \exp(-E_a / RT) \tag{6}$$

where A is a constant and E_a is the activation energy. The activation energy can be used to obtain information of whether the rate-controlling step is diffusion or surface integration. A complete crystal growth expression that includes both the effect of temperature and supersaturation on the growth rate would, therefore, be written as:

$$G = A \exp(-E_a / RT)(\sigma + 1)^g \tag{7}$$

The agglomeration and disruption kernels are also assumed to depend on the supersaturation in power law form:

$$K_{aggl} = \beta_{aggl} f(\varepsilon)\sigma^g \tag{8}$$

$$K_{disr} = \beta_{disr} g(\varepsilon)\sigma^g \tag{9}$$

and the mean crystal residence time is:

$$\tau = \frac{Q}{V} \tag{10}$$

The method of moments, described by Hulburt and Katz [9], was used to solve PBE (a partial integro-differential equation). Using the method of moments, equation (1) becomes a set of ordinary differential equations in the moments. The j moment is:

$$\mu_j = \int_0^\infty L^j n(L) dL \tag{11}$$

The lower order moments (i.e., $j = 0,1,2,3$) are related to the physical description of the particle size distribution, i.e. μ_0 is related to the total number of particles, μ_1 is related to the total particle diameter, μ_2 is related to the total particle surface area and μ_3 is related to the total particle volume.

For a well-mixed batch reactor in which crystal breakage and agglomeration may be neglected, the population balance equation leads to the partial differential equation which describes the crystal size distribution n(L, t) as a function of both crystal size and time, where G is the overall linear growth rate (dL/dt); equation (1) becomes:

$$\frac{\partial n}{\partial t} + \frac{\partial (Gn)}{\partial t} = 0 \tag{12}$$

For example, if the crystal growth rate is invariant with size and in the absence of particle breakage and agglomeration, after the moment transformation equation (12) is represented by a set of ordinary differential equations (ODEs) in terms of the moments:

$$\begin{aligned} \frac{\partial \mu_0}{\partial t} &= 0 \\ \frac{\partial \mu_1}{\partial t} &= G\mu_0 \\ \frac{\partial \mu_2}{\partial t} &= 2G\mu_1 \\ \frac{\partial \mu_3}{\partial t} &= 3G\mu_2 \end{aligned} \tag{13}$$

$$c(t) = c(0) - \rho_c k_v \mu_3(t) \tag{14}$$

In order to model the time-dependent behavior of a continuous system, the mass balance (eq. 14) was solved together with eq. (5) over an interval of time. The values for g and k_g were obtained from a least – squares optimization.

RESULTS AND DISCUSSION

In Table 1 is presented the variation of the final particle mean diameter with concentration and temperature. When precipitation takes place at lower concentrations, the nucleation rate is slowly, the growth rate is faster (the diffusion phenomena become important in the process) and the particles grow. At higher concentrations the nucleation rate is faster, stabile nuclei are formed and no changes in the particle diameter are observed.

In a precipitation process, crystal size distribution depends on the $\frac{\textit{growth rate}}{\textit{nucleation rate}}$ ratio. At 20 ^{0}C the growth rate is slower, in the first stage many critical nuclei are formed, and then they simply redissolve because they are extremely unstable. At 50 ^{0}C the growth rate is faster, the number of the critical nuclei formed is insignificant so that the nuclei grow beyond a certain critical size and become stable.

The analysis of CSD (Figure 1 – (a) and (b)) using the population density data from the Counter Coulter exhibits almost oscillating behavior due to the agglomeration and particle disruption.

Table 1. Mean particle diameter at different work conditions

$C_{Ca_3(NO_3)_2}$ **[mol/l]**	$C_{(NH_4)_2HPO_4}$ **[mol/l]**	**Mean particle diameter [μm]**	
		20 ^{0}C	50 ^{0}C
1.25	0.46	0.02	0.02
1	0.4	0.02	0.02
0.67	0.3	4.61	0.02
0.5	0.24	5. 33	0.02
0.29	0.15	6. 13	0.02
0.15	0.09	6. 17	0.02

First it increases to a maximum and then decreases, eventually approaching steady state after 22 hours. This behavior could be observed for all concentrations and temperatures (only the representative concentrations were presented in this article).

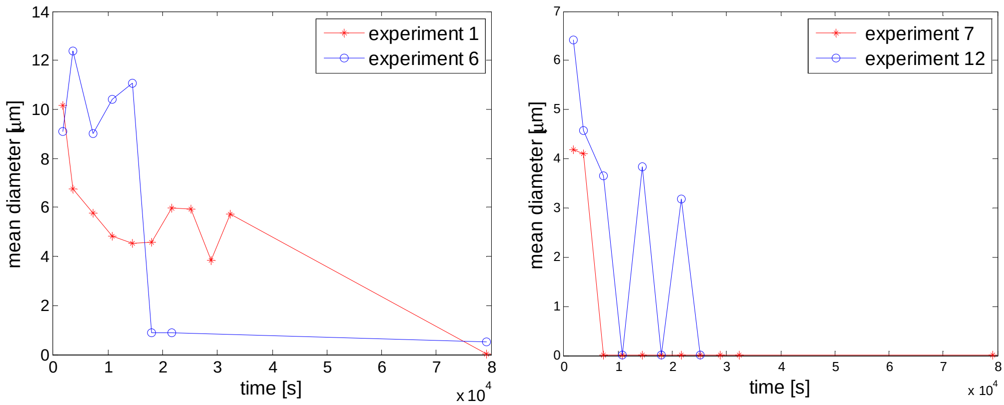

(a) **(b)**

Figure 1. Mean particle diameter vs time at 20 ^{0}C (a) and 50 ^{0}C (b)

According to the first law of precipitation, with progressively increasing concentration of the reacting solutions, the mean magnitude of the individual crystals of precipitates will pass through a maximum. As the time becomes greater, this maximum is displaced to the left side and upwards [10]. Figure 2 shows the initial particle size distribution and the distribution after 5 h of stirring (a semi-log graph, defined by a logarithmic scale on the x axis, and a linear scale on the y axis). The distribution gradually shifts to smaller sizes as large particles are reduced in size by breakage or attrition.

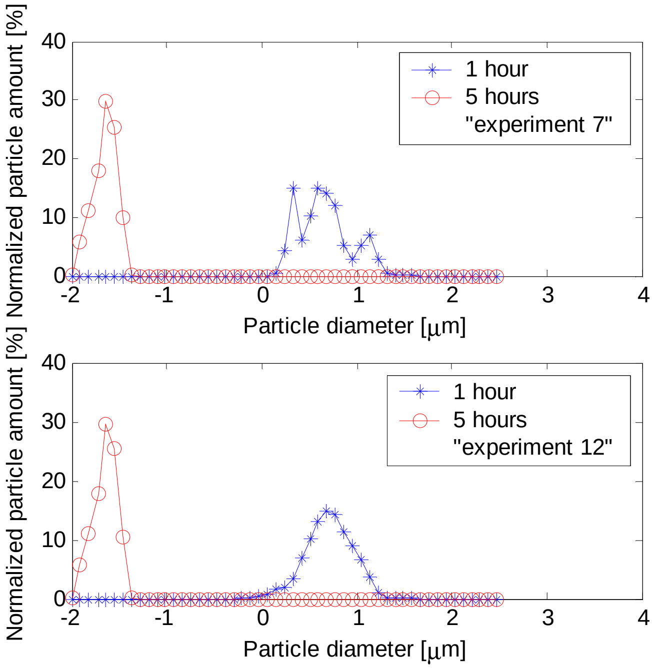

Figure 2. Number density

Furthermore, the measured total number of particles increases as each breakage event leads to a number of daughter particles (this behavior was observed at all range on concentration presented in Table 1).

The growth rate can be directly determined from the third moment, assuming that size-independent growth and the third moment (mass) is conserved in the agglomeration and disruption process. Knowing the moments of the distribution, growth rate G can be calculated from:

$$G = \frac{\mu_3}{3\mu_2 \tau} \tag{15}$$

In Figure 3 – (a) and (b), the growth rate was plotted versus the time for 2 concentrations and 2 temperatures.

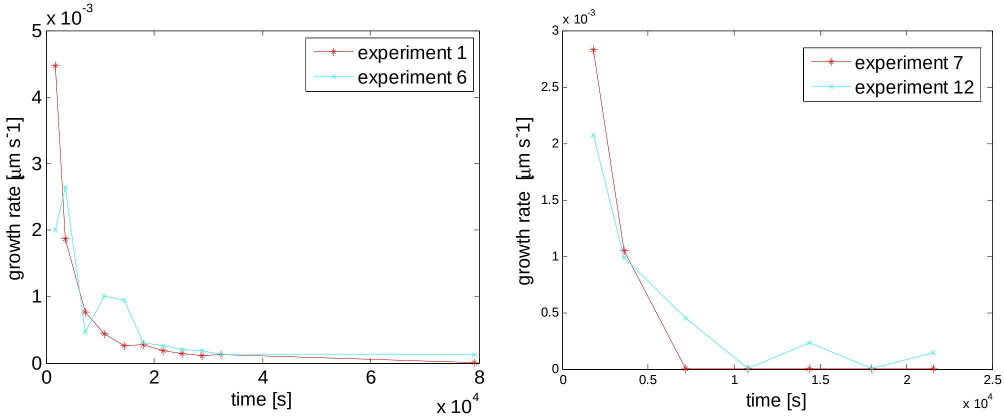

(a) **(b)**

Figure 3. Growth rate vs time at 20 ^{0}C (a) and 50 ^{0}C (b)

First an increase of the growth rate with time was observed for all conditions. The particles are agglomerating, as can be expected from the higher levels of supersaturation in the precipitation reactor. These aggregates continue to agglomerate by forming interparticle bonds. Then, due to breakage or attrition processes, a decrease was observed.

By combining the process model with an optimization algorithm the growth kinetics mechanism and parameters can be extracted from the experimental data. In Figure 4 –(a) and (b), the experimental growth rates were correlated with the growth rates obtained from the model predictions. It could be observed that the values obtained from the experiments were within the range of the simulation data. It should be considered that direct comparison of the kinetic data is not always possible.

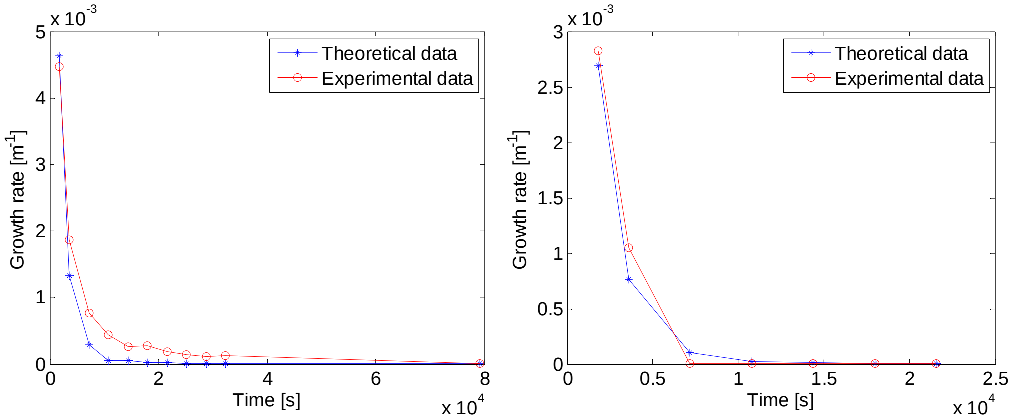

(a) **(b)**

Figure 4. Experimental and simulated growth rate vs time at (a) 20^{0}C and (b) 50^{0}C

Table 2. The values for the growth parameters

Experiment	g	k_g
1	1.79	$9.0 \cdot 10^{-13}$
2	1.68	$4.1 \cdot 10^{-12}$
3	1.92	$3.0 \cdot 10^{-13}$
4	1.95	$3.0 \cdot 10^{-13}$
5	1.95	$3.0 \cdot 10^{-13}$
6	1.98	$3.0 \cdot 10^{-13}$
7	1.74	$1.1 \cdot 10^{-12}$
8	2	$1.0 \cdot 10^{-13}$
9	1.90	$3.0 \cdot 10^{-13}$
10	1.54	$1.0 \cdot 10^{-13}$
11	1.83	$9.0 \cdot 10^{-13}$
12	1.98	$3.0 \cdot 10^{-13}$

Using an optimization algorithm based on a least squares minimization the growth parameters g and k_g from equation (5) were determined and the values are presented in Table 2. From the theoretical considerations, for diffusion controlled growth g = 1, for crystal growth originating from screw dislocations g = 1 - 2 and for polynuclear growth g > 2.

CONCLUSIONS

For the obtaining process of hydroxyapatite, a technique already known for other systems was used to determine the growth kinetics from experimental precipitation data (CSD). The model was able to predict reasonably well the growth rates for different work conditions (concentrations and temperatures) and can also be used to analyze experimental data from crystallization.

The results presented demonstrate that in the batch precipitation experiments is a strong dependence of the crystal size distributions on the feed concentrations and temperature. Due to this fact, small particles could be obtained at higher temperatures and supersaturations. Because the aggregation/growth rate increases with the supersaturation and the disruption rate increases with higher rotational speeds, further experiments are needed in order to show the dependence of the crystal size distribution on the mode of mixing.

EXPERIMENTAL SECTION

Hydroxyapatite was precipitated from reacting supersaturated solutions of calcium nitrate and bi-ammonia phosphate, at $pH = 11$ [11], according to the following equation:

$$10Ca(NO_3) + 6(HN_4)_2HPO_4 + 6NH_4OH + 2NH_3 \rightarrow Ca_{10}(PO_4)_6(OH)_2 + 20NH_4NO_3 + 6H_2O \quad (16)$$

To investigate the precipitation kinetics, the experiments were carried out under different feed concentrations and two temperatures (the values are presented in Table 3). At different preset times (see the plots), samples were taken and analyzed by laser light scattering technique using a Counter Coulter WING-SALD 7101.

Table 3. Experimental conditions (temperatures and feed concentrations)

Experiment		$C_{Ca_3(NO_3)_2}$ [mol/l]	$C_{(NH_4)_2HPO_4}$ [mol/l]
20 ^{0}C	50 ^{0}C		
1	7	1.25	0.46
2	8	1	0.4
3	9	0.67	0.3
4	10	0.5	0.24
5	11	0.29	0.15
6	12	0.15	0.09

NOTATIONS

B_{aggl} birth rate due to agglomeration, m^{-4} s^{-1}
B_{disr} birth rate due to disruption, m^{-4} s^{-1}
C concentration of the reactant, g, mol m^{-3}
D_{aggl} death rate due to agglomeration, m^{-4} s^{-1}
D_{disr} death rate due to disruption, m^{-4} s^{-1}
g kinetic order of growth, dimensionless
G molecular growth rate, m s^{-1}
k_v volumetric shape factor
K_g growth rate coefficient, m s^{-1}
K_{aggl} agglomeration rate, m^3 s^{-1}
K_{disr} disruption rate, s^{-1}
K_{sp} solubility product, mol^2 m^{-6}
L particle size, m
n population density, # m^{-4}
Q flow rate, m^3 s^{-1}
S (relative) supersaturation, dimensionless
t time, s
V reactor volume, m^3

Greek letters

μ_j	j^{th} moment of distribution, m^{j-3}
β_{aggl}	agglomeration kernel
β_{disr}	disruption kernel
ε	power input per unit volume, W kg^{-1}
ρ	suspension density, g/l
σ	(absolute) supersaturation (S-1), dimensionless
τ	mean residence time, s

REFERENCES

1. R. Barabás, A. Pop, E. Fazakas, V. Dejeu, *Proc. 10th ECerS Conf.,* Göller Verlag, Baden-Baden, **2007**, 925.
2. N. Ellis, A. Margaritis, C.L. Briens, M.A. Bergougnou, *AIChE Journal*, **1996**, *42*, 87.
3. H.M. Hulburt, S. Katz, *Chem. Eng. Sci*., **1964**, *19*, 555.
4. A. Jones, “Crystallization Process Systems”, **2002**, chapter 5.
5. S. Koutsopoulos, *Langmuir*, **2001**, *17(26*), 8092.
6. C.L. Kibby, W.K. Hall, “The Chemistry of Biosurfaces Vol. 2”, M.L. Hair ed., Dekker, New York, **1972**, 663.
7. J.O. Leckie, W. Stumm, “In the changing chemistry of the oceans”, D. Dyrssen and D. Jagner, Eds. Almquist and Wiksell, Stockholm, **1972**.
8. P.P. von Weimarn*, Chem. Rev.,* **1926**, *2,* 217.
9. D. Ramkrishna, *Reviews in Chemical Engineering*, **1985**, *3(1),* 49.
10. A.D. Randolph, M.A. Larson, “Theory of Particulate Processes, 2nd ed.”; Academic Press: San Diego, CA, **1988**.
11. R. Zauner, A. Jones, *Chem. Eng. Sci*., **2000**, *55*, 4219.